

A low-speed high-torque permanent magnet synchronous motor - Reducing cogging torque and eddy current loss -

Taichi Nakamura^{*1}, Takafumi Koseki^{*1}, and Yasuaki Aoyama^{*2}

Various electric propulsion systems are used in the industrial field. Recently permanent magnet type synchronous motor (PMSM) is focused on due to several advantages. One of them is producing high torque, so this capability is suitable to direct drive. The application to electric ships requires motors with high torque at low speed. Such requirement was the motivation for the design of a new PMSM, and a transverse flux type PMSM was investigated in the previous research. However this motor had two problems. One was high cogging torque. The other was eddy current loss in the disk. The authors propose a new design to reduce cogging torque with the use of pole-core combination. In addition the material of the disk has been changed to reduce eddy current loss. Finally the characteristics of the newest prototype motor are explained.

Keywords: permanent magnet synchronous motor(PMSM), transverse flux machine (TFM), cogging torque, pole-slot combination, eddy current loss.

1 Introduction

High-thrust electric motors are a significant component in many modern industrial and consumer applications. Recently a permanent magnet synchronous motor(PMSM) has been gaining popularity in the industrial field because a PMSM has some advantages such as large output in spite of small size compared with other traditional motors. That characteristics allows the application in direct drive systems.

High torque direct drive motors can offer various advantages, such as reduced noise and vibration due to the absence of mechanical gear or transmission. Therefore advantages in direct drive machine technology are crucial for improving motor systems in applications such as electric cars, and one important industrial application for direct drive motors is electric ships. The motors for ships require high torque at low speed, therefore the transverse flux machine is suitable to direct drives for electric ships. In previous research the transverse flux type PMSM for ships was investigated[1][2][3]. However there were two problems to be solved. One was high cogging torque that causes noise or vibration. The other was eddy current loss in the disk of the rotor.

The authors propose a new design to solve the above problems. In this paper the configuration to reduce cogging torque with the use of pole-core combination is described circumstantially. Also, the material of the disk has been changed in order to reduce eddy current loss. Finally the specification of the newest prototype motor is described comparing with the previous prototype motor.

Correspondence: Taichi Nakamura, Department of Electrical Engineering and Information Systems, Graduate School of Engineering, The University of Tokyo, 7-3-1, Hongo, Bunkyo-ku, Tokyo, 113-8656, Japan (e-mail: t_nakamura@koseki.t.u-tokyo.ac.jp)

^{*1} The University of Tokyo, ^{*2} Hitachi Research Laboratory

2 C-core type transverse flux type PMSM

2.1 Transverse flux type PMSM

The transverse flux type PMSM, introduced by Weh, Hoffmann, and Landrath in [4] is the most recent major evolution in PMSMs for direct drives. The transverse flux machine takes advantages of a three-dimensional flux path. This is different from either the radial or axial flux type motors where the electrical and magnetic loading of the machine must tradeoff for space. The configuration of the TFM is shown in Fig.1.

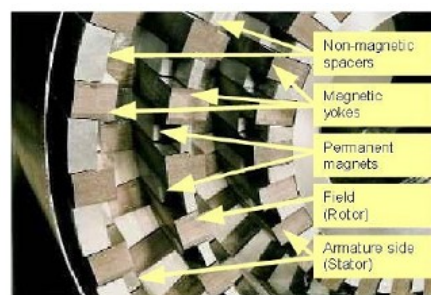


Fig.1 Original TFM by Weh[4]

Also Hitachi's Tunnel Actuator (TA) for linear drive applications can produce high thrust with a similar flux path configuration[5].

2.2 C-core type transverse flux motor

The C-core type transverse flux motor with the idea of the TA structure in Fig.2 was investigated through the use of electric ships[1][2][3]. The remarkable characteristic in the motor was 38 magnets and 18 cores combination with the expectation of high-torque[3]. However there were two problems that needs to be solved. One was high cogging torque, and the other was eddy current loss in the disk.

Cogging torque is often observed in PMSMs. It causes excessive noise and harmful vibration to the machine. Skewing method was employed to reduce cogging torque in the previous prototype motor (2nd prototype). However high cogging torque was generated and the motor could not rotate smoothly. It was 3.5Nm by finite element method, and that was 1/9 of rated torque. For this reason another method to reduce cogging torque must be discussed.

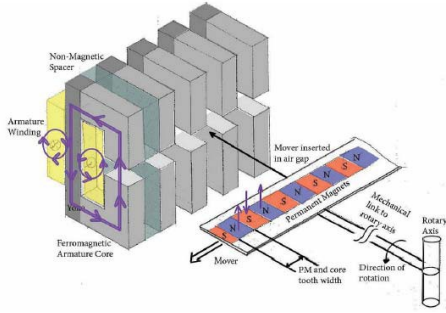


Fig.2 Flux path through the C-core and the magnet

The temperature of the rotor disk made from stainless steel rose through continuous drive for 30 minute. The authors guessed that the reason could be eddy current loss in the support material, i.e., stainless steel. Fig.3 shows the measurement result of the each loss under no load running when driving frequency is 35 Hz.

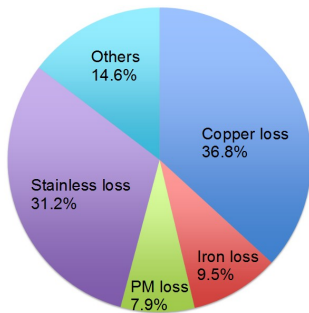


Fig.3 Empirical losses under no load operation [3]

It is found that Eddy current loss in the disk accounts for 30% of total loss under no load driving. Electrical resistivity of the stainless steel used in the rotor is $7.2 \times 10^{-7} \Omega m$. Hence the rotor should be made from a material that has higher electrical resistivity with high strength such as Fiber Reinforced Plastic (FRP) in order to reduce the eddy current.

3 Design of the new C-core type transverse flux motor

3.1 Cogging torque with pole-core combination

The 2nd prototype motor could not rotate smoothly because of high cogging torque. Cogging torque causes

excessive noise and harmful vibration to the machine, so the method to reduce cogging torque must be discussed. The authors take notice of pole-slot combination. The bigger the least multiple of pole and slot number, the less cogging torque. Therefore this method is often employed on a PMSM.

3.1.1 Configuration of 8 poles 9 slots combination

Fig.4 shows the configuration of the 8 poles 9 slots combination.

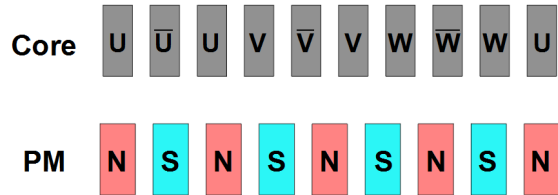


Fig.4 Linear model of 8 poles 9 slots combination

Each phase is ordered in the following sequence,

$$U, \bar{U}, U, V, \bar{V}, V, \bar{W}, W \text{ and } U.$$

Therefore the concentrated windings must be employed on the slots in 8 poles 9 slots combination.

The value of the magnetomotive force by the armature is important to obtain high torque in the design of PMSMs. To avoid the spacial constraint of the winding turns, windings were wound around three cores of which phases were the same in the 2nd prototype motor. However each winding must be concentrated in 8 poles 9 slots combination. The authors propose the novel configuration in which windings are wound around three cores keeping the same configuration of magnets and cores in 8 poles 9 cores combination.

3.1.2 Proposed magnet-core combination

The number of the U phase is different from the number of the \bar{U} phase in 8 poles 9 slots combination. Therefore a pair of the 8 poles 9 slots configuration are considered to make up the number of each phase as shown in Fig.5.

All cores are labeled to distinguish between them as shown in Fig.5. Each core position in electrical degrees from the nearest N-pole magnet was discussed with keeping the original 8 magnets 9 cores combination as shown in Fig.4. Table 1 shows each core position from the nearest N-pole magnet. Next each core is ordered so that windings are wound around three cores and phases are ordered in the following sequence,

$$U, \bar{W}, \bar{V}, \bar{U}, W, \bar{V} \text{ and } U.$$

Each core position are decided when U1 core position is 0 as shown in Table 2.

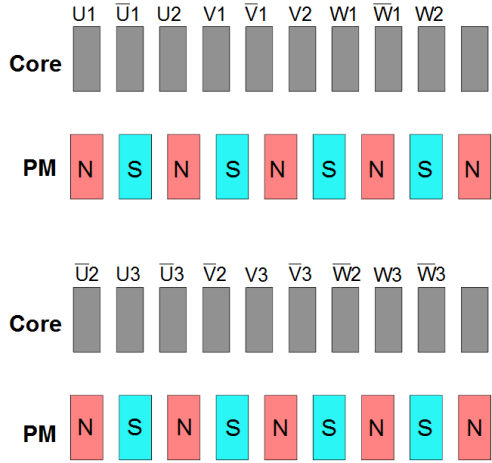


Fig.5 A pair of 8 poles 9 cores combination

Table 1 Each core position from the nearest N-pole magnet

Core name	Distance from N pole
U1	0
U2	$-2\pi / 9$
U3	$-4\pi / 9$
V1	$6\pi / 9$
V2	$4\pi / 9$
V3	$2\pi / 9$
W1	$-6\pi / 9$
W2	$-8\pi / 9$
W3	$8\pi / 9$
$\bar{U}1$	$8\pi / 9$
$\bar{U}2$	$6\pi / 9$
$\bar{U}3$	$4\pi / 9$
$\bar{V}1$	$-4\pi / 9$
$\bar{V}2$	$-6\pi / 9$
$\bar{V}3$	$-8\pi / 9$
$\bar{W}1$	$2\pi / 9$
$\bar{W}2$	0
$\bar{W}3$	$-2\pi / 9$

Table 2 Position of each core

Phase	Core 1	Core 2	Core 3
U	0	$16\pi / 9$	$32\pi / 9$
\bar{W}	$38\pi / 9$	$54\pi / 9$	$70\pi / 9$
V	$78\pi / 9$	$94\pi / 9$	$110\pi / 9$
\bar{U}	$116\pi / 9$	$132\pi / 9$	$148\pi / 9$
W	$156\pi / 9$	$174\pi / 9$	$192\pi / 9$
\bar{V}	$194\pi / 9$	$210\pi / 9$	$226\pi / 9$
U	$234\pi / 9$	$250\pi / 9$	$266\pi / 9$

That proposed configuration is suitable to obtain large amount of the armature magnetomotive force because the windings can be wound around three cores.

The number of magnets must be decided in this proposed configuration. The distance of $\bar{V}3$ core from U1 core is $226\pi/9$, and the multiples of 2π that is the nearest number of $226\pi/9$ is 26π ($=234\pi/9$). Therefore one of magnet-core combination in the proposed configuration is 26 magnets and 18 cores as shown in Fig.6. A constraint of $26+12n$ magnets must be there because the distance between N-pole magnets is 2π in electrical degrees and there are 6 phases. In a new design of a transverse flux type PMSM, the number of magnets has been decided as fifty for possibly short pole pitch that enable high torque. The proposed configuration which is 50 poles 18 cores combination is shown in Fig.7.

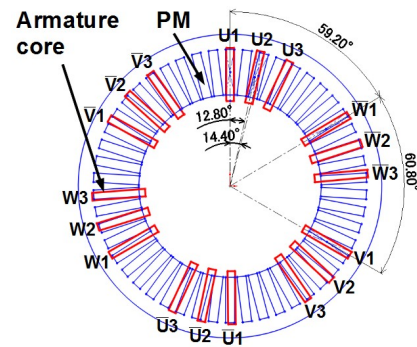


Fig.7 Proposed magnet-core combination

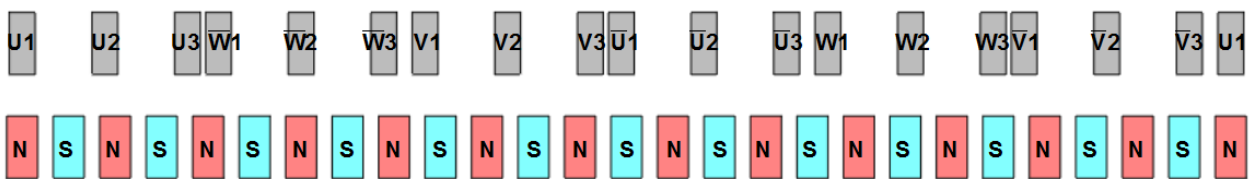


Fig.6 The proposed configuration in linear model

3.2 Core design and new material of the disk

3.2.1 Core design

When the windings are wound around three same phase cores as the configuration of the 2nd prototype motor[3], flux linkage of the air gap between core tooth decreases because the magnetic circuit is generated around the space. Hence windings shall be close to the air gap so that the effective flux linkage can be maximized. Therefore the new armature core is as shown in Fig.8.

This design has another advantage, which is effectively skewed relationship between the magnet and the core tooth. That characteristics is expected to contribute to a decrease of cogging torque.

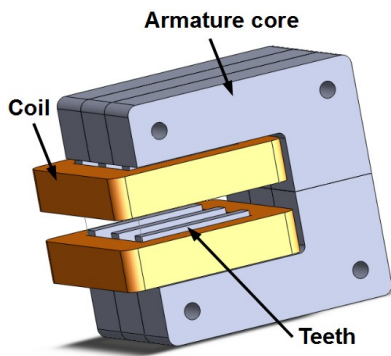


Fig.8 Design of a armature core in the proposed model

3.2.2 New material for the disk of the rotor

As already mentioned in chapter 2, eddy current loss in the rotor disk was a serious problem to be solved. Hence Carbon Fiber Reinforced Plastic (CFRP) has been employed as the material of the rotary disk. The value of the electrical resistivity of CFRP is about $0.1\Omega\text{m}$ and that is 10^5 times larger than stainless steel. Therefore eddy current can not flow and eddy current loss in the disk is drastically suppressed although the material and machining of the CFRP are rather expensive.

3.3 Analysis of the proposed model using FEM

3.3.1 Design with low cogging torque

When 8 poles 9 cores configuration is employed on a PMSM to reduce cogging torque, it is important to adjust the size of a magnet, the width of a core teeth and a pole pitch (a radius of rotation) precisely. The authors have decided the size of a magnet and the width of a core teeth in advance and adjusted a radius of rotation. The size of a magnet and a width of the core teeth are shown in Table 3.

Table 3 Magnet size and teeth width

Magnet size	6mm×30mm×5mm
Teeth width	5mm

The thickness of CFRP must be more than 1.5mm to keep the strength. Hence the authors analyzed cogging torque using FEM with this constraint when the range of a radius of rotation was from 75mm to 90mm using the model as shown in Fig.9. The maximum value of cogging torque in each case is shown in Fig.10.

It is found that when a radius of the rotation is 75mm, the maximum value of cogging torque is effectively suppressed to only 0.04Nm and that value is least of all cases. Consequently cogging torque in the proposed model is about 80 times smaller than in the 2nd prototype motor. The new design, therefore, is successful in suppressing cogging torque.

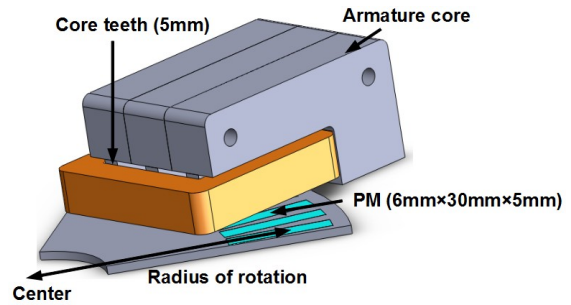


Fig.9 Proposed model for FEM analysis

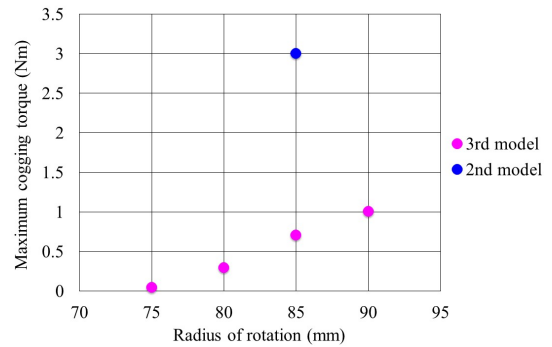


Fig.10 Numerical result of maximum cogging torque in each radius of rotation

3.3.2 Static torque analysis

It was decided that winding turns was 400 turns per core unit, and the result of static torque about U and \bar{U} phase in each case is shown in Fig.11.

The maximum value of static torque in each case is nearly the same. The following shows the important results from the analysis of cogging torque and static torque.

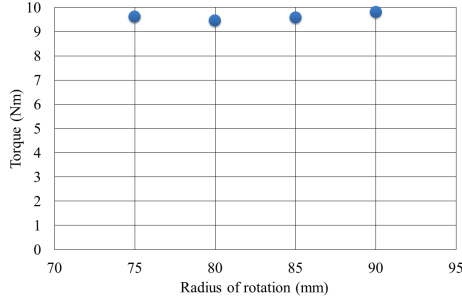


Fig.11 Numerical result of static torque in each radius of rotation

1. The maximum value of cogging torque is only 0.04Nm when a radius of the rotation is 75mm.
2. The maximum value of static torque is similar in each case.

The authors decided that a radius of the rotation was 75mm considering both these results and the process limitation of CFRP to keep its strength.

3.4 Specification of the proposed model by FEM

The specification of the proposed model is calculated when d-axis current is zero and q-axis current is 2A. Table 4 shows both specification of the proposed model and the 2nd prototype motor.

Cogging torque is expected to decrease significantly in the proposed model. In addition, power factor is improved compared to the 2nd prototype motor when d-axis current is 0, because the windings are wound near the air gap. On the other hand force density is reduced by 10% due to the decrease of the amount of magnets(21%).

Table 4 Specification of the proposed model when $i_d = 0$

Specification	Proposed model	
Winding (turns)	400	
Rated current (A)	2	
Winding resistance (Ω)	4.4	
Self inductance (H)	0.049	
	Proposed	2nd motor
Torque (Nm)	21.3	33.7
Force Density (kN / m^2)	90	99.8
Maximum cogging torque (Nm)	0.04	3.5
Power factor	0.75	0.58
Drive frequency (Hz)	35	35

4 Machine parameter characterization

4.1 Newest prototype motor with low cogging torque

The newest prototype motor(3rd prototype) based on the proposed design was manufactured as shown in Fig.12. However the winding turns were altered to 334 turns per core unit because of space constraint.

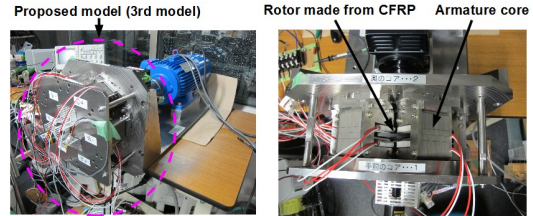


Fig.12 The newest prototype motor

The rotation of the motor in open circuit was as smooth as expected. This result means successful suppression of cogging torque in the proposed magnet core combination.

4.2 Experimental results

4.2.1 Armature resistance and self-inductance measurements

The armature resistance per core unit was measured using a DC-voltage drop test. The armature resistance per core unit was 4.03Ω from the experiment.

The self-inductance per core unit was measured using a AC-voltage source. The experimental result is shown in Fig.13.

It is found that the self-inductance per core unit is 40mH.

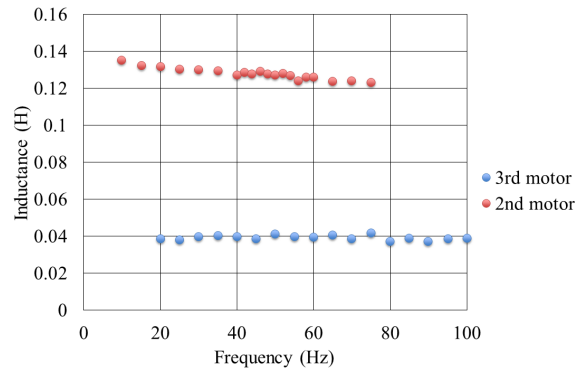


Fig.13 Self inductance measurement

It is difficult to distinguish the d-axis from q-axis visually in the 3rd prototype motor. However the d-axis inductance is almost the same as the q-axis inductance

considering the magnet circuit calculation. Therefore both inductance can be calculated using this result.

The frequency dependence of the self-inductance must be noted in Fig.13. The self-inductance decreases as frequency increases in the 2nd prototype motor because eddy current which causes the effect of magnet screen is generated in the disk made from stainless steel. On the other hand, the self-inductance in the 3rd prototype motor remains constant as frequency increases. The authors guess that the flow of eddy current is prevented by using CFRP from the result.

4.2.3 Specification of the 3rd prototype motor

The authors estimate the specification using the experimental results when d-axis current is zero and q-axis current is 2A. The estimated specification of the 3rd prototype motor and the specification of the 2nd prototype motor is shown in Table 5.

It is found that power factor is improved compared to the 2nd prototype motor when d-axis current is zero. That is because the windings are wound around the air gap. However force density decreases to 71.5kN/m² due to the decrease of winding turns to about 80% of the initial turns with the space constraint. Also the maximum output torque is 16.9N and that value is only 1/6 of the torque of commercial motors with similar size. This is because the space-utility factor is low in the 3rd prototype motor as shown in Fig.12. Therefore the space utility-factor should be maximized for larger output torque.

Table 5 Specification based on empirical data in the 3rd prototype motor

Specification	3rd motor	2nd motor
Armature resistance (Ω)	4.0	5.1
Winding turn	334	400
Self inductance (H)	0.035	0.137
Induced internal voltage (V)	24.7	32.5
Torque (Nm)	16.9	33.7
Force density (kN/m ²)	71.5	99.6
Power factor	0.79	0.58
Drive frequency (Hz)	35	35

5 Conclusion

A new design of a disk-rotor type transverse flux machine to reduce cogging torque and eddy current loss has been described in this paper.

It is significant that cogging torque is reduced easily by applying the pole-core (slot) combination such as 8 poles 9 cores combination. A considerable decrease of cogging torque to only 0.04Nm was achieved in the

proposed motor. In addition, the result of the frequency dependency of the self-inductance measurement shows that eddy current loss is decreased due to employing CFRP to the disk of the proposed motor. Windings should be wound around core teeth as close as the air gap in order to increase flux linkage of the air gap. This method contributes to an improvement of power factor.

As future works, at first the authors will control the 3rd prototype motor when d-axis current is zero, and verify the specification of the motor. The quantitative evaluation of each loss including eddy current loss in the disk by experiment also should be done.

In spite of the improvements, higher torque was not achieved in the 3rd prototype motor compared to existing industrial products of high torque motors such as axial flux motors. Therefore substantially better space utility shall be investigated in a next design. The authors will design a new model with careful consideration of the effective utilization of the space.

Acknowledgment

We would like to thank MT-Drive (MTD) and Japan Society for the Promotion of Science (JSPS) for their friendly support to this research.

References

- [1] G. Patterson, T. Koseki, Y. Aoyama, and K. Sako, "Simple Modeling and Prototype Experiments for a New High-Thrust, Low-Speed Permanent Magnet Disk Motor", Proc. 12th International Conference on Electrical Machines and Systems, Tokyo, Japan. Nov 2009.
- [2] K. Sato, J.S. Shin, T. Koseki and Y. Aoyama, "Basic Experiments for High-Torque, Low-Speed Permanent Magnet Synchronous Motor and a Technique for Reducing Cogging Torque", International Conference on Electrical Machines, Roma, Italy, Sep 2010.
- [3] K. Sato, T. koseki, and Y. Aoyama, "Design and Verification of Permanent Magnet Synchronous Motor for High Torque Drive at Low Speed", RM-10-147(In Japanese reviewing)
- [4] Weh, H., Hoffman, H., Landrath, J., "New Permanent Magnet Excited Synchronous Machine with High Efficiency at Low Speeds", Proceedings of the International Conference on Electrical Machines, 1988.
- [5] Kim, H.J., Nakatsugawa, J., Sakai, K., Shibata, H., "High-Acceleration Linear Motor, "Tunnel Actuator", The Magnetics Society of Japan, Vol. 29, No. 3, pp 199-204, 2005.